

element and a Fourier expansion in the circumferential direction. The predictions sum seven modes ($n=0$ to $n=6$) and comparisons of the measured and predicted strains are shown in Figs. 3a and b. Bending strain response is dominated by the fundamental bending mode ($n=2$) and has lower amplitude, higher frequency modes superimposed.

As indicated in Fig. 3, excellent agreement is found between measured and predicted strains for this experimental setup. These simple structural experiments are used in our laboratory to select reasonable flyer plate designs and flyer-to-shell air gaps before testing full-scale systems.

References

- ¹Benham, R. A. and Mathews, F. H., "X-Ray Simulation with Light-Initiated Explosive," *The Shock and Vibration Bulletin*, Bulletin 45, Oct. 1974, pp. 21-22.
- ²Lindberg, H. E. and Kennedy, T. C., "Dynamic Plastic Pulse Buckling in Beyond Strain-Rate Reversal," *Journal of Applied Mechanics*, Vol. 42, No. 2, June 1975, pp. 411-416.
- ³Bealing, R., "Impulse Loading of Circular Rings," *Experimental Mechanics, Proceedings of the 11th Annual Symposium*, University of New Mexico, 1971, pp. 15-26.
- ⁴Forrestal, M. J. and Overmier, D. K., "An Experiment on an Impulse Loaded Elastic Ring," *AIAA Journal*, Vol. 12, May 1974, pp. 722-724.
- ⁵Tucker, W. K., "Two Digital Computer Programs for Flyer Plate-Capacitor Bank Analysis," SC-DR-70-122, April 1970, Sandia Laboratories, Albuquerque, N. Mex.
- ⁶Stricklin, J. A., Haisler, W. E., and Von Riesenmann, W. A., "Large Deflection Elastic-Plastic Dynamic Response of Stiffened Shells of Revolution," *Journal of Pressure Vessel Technology*, Vol. 96, Series J, May 1974, pp. 87-95.

Expansion Tube With Nozzle Plate: Theory and Experiment

F. H. Oertel Jr.,* N. Gerber,*

and

J. M. Bartos†

U. S. Army Ballistic Research Laboratories,
Aberdeen Proving Ground, Md.

Introduction

THE expansion tube uses unsteady expansion to generate high-enthalpy high-velocity flows of test gases initially isolated in the driven section by the first and second diaphragms (Fig. 1)—on one side against the high-pressure driver gases and on the other against the evacuated expansion section. The BRL expansion tube has been used to make measurements in nonequilibrium shock layers as selected gases flowed past axisymmetric bodies. For those experiments, it was desirable to have a freestream flow uniform in density and velocity with low dissociation and low impurity level.

An earlier paper¹ reported extensive investigations of test flow characteristics in our original expansion tube (using simply-supported mylar second diaphragms) and preliminary results in the modified tube (using scribed metal second diaphragms placed adjacent to a perforated plate, called a nozzle plate.²) Test flows in the original tube were found to be quite uniform for the most part—density fluctuations were

typically less than $\pm 15\%$.³ However, it appeared that with the nozzle plate the flow could be made more uniform (and more contamination-free) by forcing the diaphragm to petal open along the scribes into the holes of the nozzle plate; and model and instrumentation damage could be reduced, since the nozzle plate blocks first diaphragm particles.

The purpose of this paper is to present results of computations of test flow properties which supplement limited preliminary data^{1,2} and, for the first time, to evaluate the computation model by experimental results. In our experiments, we use a new nozzle plate design suggested by the results of Refs. 1 and 2.

Computations

We adopted the operation cycle for the modified expansion tube shown in the $x-t$ diagram of Fig. 1. For the computations we assumed that: 1) diaphragms open ideally; 2) expansion waves are isentropic centered rarefactions; 3) one-dimensional conservation equations for an inviscid, non-conducting, diatomic gas in vibrational and chemical equilibrium are valid; 4) steady quasi-one-dimensional flow in a single nozzle with an effective area ratio, A/A^* , is applicable (A = cross-sectional area of expansion tube, A^* = sum of nozzle throat areas); and 5) the first shock is fully reflected from the second diaphragm before the diaphragm opens.

The governing equations are given in Ref. 4, and the numerical-graphical procedure used to solve them is outlined there. Flow properties in each section of the expansion tube were computed for the following range of parameters: 1) first shock Mach number, M_{s1} : 3-9; 2) initial pressure in the driven section, P_1 : $2.76 \times 10^4 \text{ N/m}^2$ – $8.28 \times 10^4 \text{ N/m}^2$; 3) initial pressure in the expansion section, P_{10} : 6.66 N/m^2 – 26.7 N/m^2 ; 4) effective nozzle area ratio, A/A^* : 2 (new nozzle plate)⁵ and 4 (first nozzle plate)²; 5) initial temperatures in driven and expansion sections, T_1 and T_{10} : 300°K.

From an operational standpoint, the most important properties of the test gas are the density ρ_s and the velocity u_s in the test section. They are plotted in Fig. 2 for the new nozzle plate ($A/A^* = 2$). Each symbol gives the result of a computation for real air and a discrete set of initial parameters. The degree to which initial parameters affect properties in the test section is summarized in Table 1.

Experimental Measurements and Techniques

The experimental measurements and techniques used here have been described in detail.^{1,3} Detailed descriptions of the

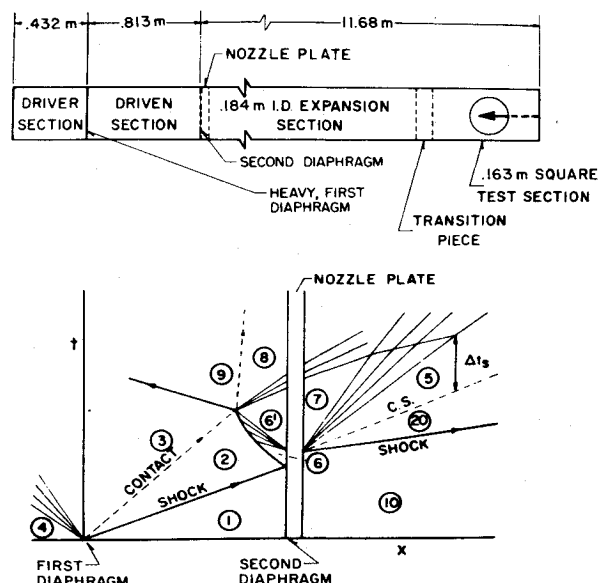


Fig. 1 Sketch of modified expansion tube and $x-t$ diagram showing full reflection of first shock.

Received February 14, 1975.

Index categories: Supersonic and Hypersonic Flow; Research Facilities and Instrumentation.

*Aerospace Research Engineer. Member AIAA.

†Mathematician.

Table 1 Effect of initial parameters on flow in test section

Test property	Strong function of:	Weak function of:
ρ_5	P_{10}, P_1	M_{s1}
u_5	M_{s1}	P_1, P_{10}
p_5	P_{10}, M_{s1}	P_1

Table 2 Percentage of useful tests

Driver mode	Second diaphragm	No. of runs	% of runs useful ^a
Cold He	0.51mm Al, scribed	10	90
Combustion-heated He	0.51mm Al, scribed	34	70
Combustion-heated He	0.81mm Al, scribed	47	95

^aThe criterion for useful test time was that the pitot pressure not deviate more than $\pm 10\%$ from the average for at least 50 μsec .

original and modified BRL expansion tubes can be found in Refs. 1 and 6; significant dimensions are shown in Fig. 1. Work with a nozzle plate^{1,2} ($A/A^* = 4$) which was made by counter-boring conical nozzles in a plate showed that it was desirable to: 1) increase the throat area; i.e., decrease A/A^* , and 2) reduce the stresses at the root of each petal by having them open along a straight hinge. A new nozzle plate ($A/A^* = 2$), consisting of many nozzles of square cross-section which diverge slightly in the stream-wise direction, was designed to incorporate these changes. The diaphragms were annealed aluminum and were scribed by hand. Several diaphragm materials and thicknesses were tried.

Commercial grade dry air was isolated in the driven section for all tests; the expansion section was evacuated. Low-velocity test flows were generated using a cold helium driver. For high-velocity flows, a combustion-heated helium driver was used. For each test we recorded: 1) initial pressures in the driver, driven, and expansion sections, 2) barometric pressure, and 3) ambient temperature. For the combustion-heated driver, a "bar"-type gage mounted in the wall of the driver monitored the pressure-history during combustion.

Oscilloscope traces of static pressure-history in the driven and expansion sections were recorded for electrically-isolated piezo-electric pressure gages mounted in the wall at several locations. Shock velocity was also obtained from these traces. Pitot pressure was measured in the test section as a function of time using a calibrated "bar"-type gage mounted at the stagnation point of a 38mm diam hemisphere cylinder model sting-mounted in the test section. Examples of the previous traces are shown in Ref. 5.

Useful test time was found in a large majority of runs, as summarized in Table 2. We were able to improve the 70% figure in Table 2 to 87% for the last 15 runs by scribing the thinner diaphragms more carefully, but the use of a thicker diaphragm for the combustion-heated driver mode was clearly indicated. The percentage of useful tests quoted for the first nozzle plate¹ was 70%.

Comparison of Computations and Experiment

Typical agreement between the computations and experiment for the new nozzle plate is shown in Fig. 3. In Fig. 3a, we show the ratio of measured shock velocity to the computed value as a function of measured freestream velocity u_5 . The agreement here is within $\pm 10\%$ for all cases. Good agreement was expected since the shock wave speed in the test section U_{s10} can be measured within $\pm 3\%$, and its computed value is insensitive to the choice of computation model.^{1,5} Figure 3b shows the ratio of measured to computed pitot pressure p_o (or density, since for hypersonic flow $p_o \approx K\rho_5 U_{s10}^2$; $K \sim 1$ for air,⁶ as a function of measured velocity in the test section for the same initial conditions as for Fig. 3a.

- $\circ P_1 = 2.76 \times 10^4 \text{ N/m}^2$
 $\square P_1 = 4.13 \times 10^4 \text{ N/m}^2$
 $\triangle P_1 = 5.51 \times 10^4 \text{ N/m}^2$
 $\nabla P_1 = 6.89 \times 10^4 \text{ N/m}^2$
 $\diamond P_1 = 8.28 \times 10^4 \text{ N/m}^2$
- $\text{--- } P_{10} = 26.7 \text{ N/m}^2$
 $\text{--- } P_{10} = 20.0 \text{ N/m}^2$
 $\text{--- } P_{10} = 13.3 \text{ N/m}^2$
 $\text{--- } P_{10} = 6.66 \text{ N/m}^2$

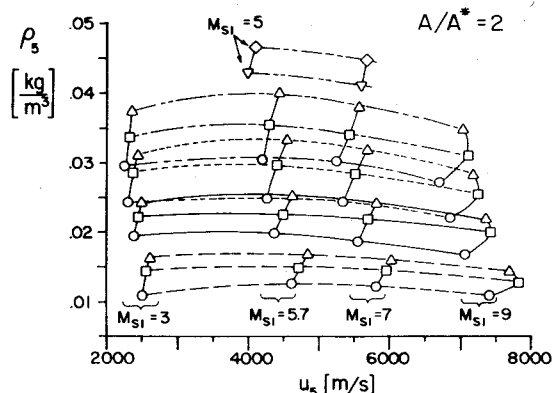


Fig. 2 Summary of density and velocity computations for real air in the test section for the new nozzle plate ($A/A^* = 2$).

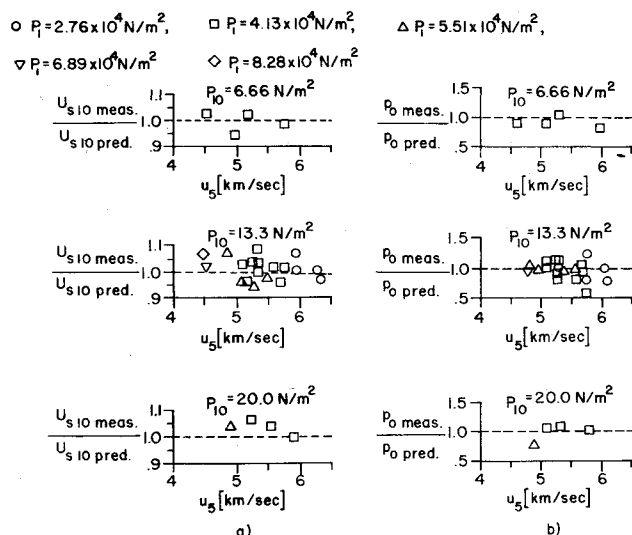


Fig. 3 Typical comparisons of measurements with computations: a) shock velocity in test section; b) stagnation pressure in test section.

The numerator is a time-averaged value for the useful test region measured from the oscilloscope traces. In general, agreement is within $\pm 20\%$; however, a bias is seen outside the error limits stated, most likely due to problems⁵ in reading P_{10} . A stronger bias was seen when measured and computed static pressure were compared (not shown); measured pressure was usually higher, often by 50% or more. Fortunately, P_{10} need not be known accurately for most experiments; it can be computed from p_5 , the measured static pressure, if needed.

The gages located in the driven section as suggested by the experience of Refs. 1 and 2 allowed the velocity of the first shock wave and the pressure behind it to be measured, so that computations could be compared with experiment for the first time. They also showed that the attenuation of the reflected first shock postulated in Fig. 1 is correct. Measured and computed reflected properties were not compared, since the choice of a reflection model—full or partial—has little practical significance.⁴

The test times measured in the original expansion tube¹ were not noticeably different from those measured in the

modified facility where it appears that the first shock is fully reflected. These observations imply that the cycle first assumed for the original expansion tube—unreflected first shock—should be modified to include reflection of the first shock.

Test times predicted for the modified facility were shorter than observed times. An explanation of this result is that computed test time is very sensitive to velocity in the test section. For example, if a U_{s10} of 5000 m/sec is increased by only 2.5% (within experimental accuracy), the estimated test time is doubled.⁴

Conclusions

Specific conclusions based on this work are: 1) A high percentage of useful test runs was found in the modified expansion tube using the new nozzle plate (Table 2); 2) The computation model chosen for the modified expansion tube is satisfactory for the range considered here; and 3) It may be inappropriate to assume that the first shock is not reflected from the mylar second diaphragm as had been done in the work on the original expansion tube.

An overview of tests made in our expansion tube leads to the following general remarks: 1) A post-run inspection of diaphragms showed that they opened more cleanly with no measurable loss of diaphragm material more often for the new nozzle plate than for the first nozzle plate; and pitot pressure and density (streak interferometry) measurements showed that the percentage of useful tests was higher for these tests (Table 2) than for tests in either the original expansion tube or the modified tube with the first nozzle plate; 2) Velocity, density, pressure, and testing time measured in the modified expansion tube are comparable to those measured in the original expansion tube; 3) Dissociation computed in the modified expansion tube (full reflection of first shock) is much lower than in similar flow facilities at the same velocity; e.g., shock tunnels; but it can become a factor at flow velocities above ~5500 m/sec⁵; and 4) Radiation measurements⁷ and measured relaxation times in Argon⁸ indicate that the total impurity level in the modified expansion tube (a few hundred parts per million) is somewhat lower than in the original expansion tube.

References

- ¹Spurk, J.H., Gion, E.J., and Sturek, W.B., "Investigations of Flow Properties in an Expansion Tube," AIAA Paper 68-371, San Francisco, Calif., 1968. Also BRL Rept. 1404, June 1968, AD 673109, U.S. Army Ballistic Research Lab., Aberdeen Proving Ground, Md.
- ²Spurk, J.H., Gion, E.J., and Sturek, W.B., "Modified Expansion Tube," *AIAA Journal*, Vol. 7, Feb. 1969, pp. 345-346.
- ³Spurk, J. H. and Bartos, J.M., "Interferometric Measurement of the Nonequilibrium Flow Field Around a Cone," *Physics of Fluids*, Vol. 9, July 1966, pp. 1278-1285.
- ⁴Gerber, N., and Bartos, J.M., "Operation Cycle of Expansion Tube with Nozzle Plate," BRL Memo. Rept. 1982, June 1969, AD 689540, U.S. Army Ballistic Research Lab., Aberdeen Proving Ground, Md.
- ⁵Oertel, F. H., Gerber, N., and Bartos, J.M., "The Modified Expansion Tube: Theory and Experiment," BRL Rept. 1741, Sept. 1974, AD A001551, U. S. Army Ballistic Research Lab., Aberdeen Proving Ground, Md.
- ⁶Spurk, J. H., "Design, Operation and Preliminary Results of the BRL Expansion Tube," BRL Rept. 1304, Oct. 1963, AD 630065, U. S. Army Ballistic Research Lab., Aberdeen Proving Ground, Md.; also, *Proceedings of the Fourth Hypervelocity Techniques Symposium*, Arnold Air Force Station, Nov. 1965, pp. 111-144.
- ⁷Spurk, J. H. and Gion, E. J., "Impurity Concentration in the Expansion Tube," *AIAA Journal*, Vol. 7, Feb. 1969, pp. 346-348.
- ⁸Oertel, F. H., "Measurement of Electron Concentrations in an Axisymmetric Nonequilibrium Shock Layer," BRL Rept. 1594, June 1972, AD 355679, U. S. Army Ballistic Research Lab., Aberdeen Proving Ground, Md.

Calculation of Transition Matrices

C. von Kerczek*

University of Maryland, College Park, Md.

and

S. H. Davis†

The Johns Hopkins University, Baltimore, Md.

I. Introduction

SYSTEMS of linear ordinary differential equations with periodic coefficients arise in the study of the stability of helicopter rotor blade flapping motions,¹⁻³ the instability of columns under periodic loading,⁴ the hydrodynamic stability of periodic laminar flows,⁵ and, in general, the stability of systems under parametric excitation.

Such problems reduce to the solution of a system of differential equations such as

$$\dot{y} = A(t)y \quad (1)$$

where y is an N -component vector, and $A(t)$ is an $N \times N$ matrix with coefficients having period T . The solutions are characterized in the Floquet Theorem⁶; every fundamental matrix solution $\Phi(t)$ of Eq. (1) has the form

$$\Phi(t) = P(t)e^{Ct} \quad (2)$$

where $P(t)$ is an $N \times N$ matrix of period T , and C is an $N \times N$ constant matrix. Thus the stability or instability of the null solution of Eq. (1) is determined by the real parts of the eigenvalues $\{\lambda_i\}$ of C . The fundamental matrix $\Phi(t)$ that satisfies $\Phi(0) = I$, the identity matrix, is called the *transition matrix*. Using the fact that $P(t)$ is T -periodic, one has

$$\Phi(T) = e^{CT} \quad (3)$$

The eigenvalues of C are obtained from the eigenvalues $\{\mu_i\}$ of $\Phi(T)$ by the relation

$$\lambda_i = \frac{1}{T} \ln \mu_i, i = 1, 2, \dots, N \quad (4)$$

The imaginary part of Eq. (4) is defined mod $[2\pi n/T]$. The transition matrix must be obtained by integrating system (1) for the N initial conditions $y_j^{(i)}(0) = \delta_{ij}$ where $y_j^{(i)}$ is the j th component of the i th column of Φ .

We first note that any convenient library subroutine that integrates ordinary differential equations can normally be used to obtain the matrix $\Phi(t)$. However, since such subroutines are usually written for the solution of *vector* equations, one should formulate the calculation procedure for the matrix Φ as one for the calculation of the N^2 component vector $(\Phi_{11}, \dots, \Phi_{1N}, \Phi_{21}, \dots, \Phi_{NN})$. Thus integration to obtain $\Phi(t)$ is accomplished in one sweep (instead of N separate integrations of Eq. (1)) and many evaluations of $A(t)$ are saved.

In most applications where systems such as Eq. (1) arise, a parameter space must be searched for boundaries that separate stable from unstable regions. The transition matrix

Received February 26, 1975; revision received April 14, 1975. This work was partially supported by NSF Applied Mathematics Program, Grant number GP-39933X.

Index category: Structural Stability Analysis.

*Assistant Professor, Mechanical Engineering Department; presently at David Taylor Naval Ship Research and Development Center, Bethesda, Md.

†Professor, Department of Mechanics and Materials Science.